Cross Entropy Benchmark for Measurement-Induced Phase Transitions

Yaodong Li,[1,2] Yijian Zou,[2] Paolo Glorioso,[2] Ehud Altman,[3] and Matthew P. A. Fisher[1]
[1]Department of Physics, University of California, Santa Barbara, California 93106, USA
[2]Department of Physics, Stanford University, Stanford, California 94305, USA
[3]Department of Physics, University of California, Berkeley, California 94720, USA

(Received 9 January 2023; accepted 16 May 2023; published 1 June 2023)

We investigate prospects of employing the linear cross entropy to experimentally access measurement-induced phase transitions without requiring any postselection of quantum trajectories. For two random circuits that are identical in the bulk but with different initial states, the linear cross entropy χ between the bulk measurement outcome distributions in the two circuits acts as an order parameter, and can be used to distinguish the volume law from area law phases. In the volume law phase (and in the thermodynamic limit) the bulk measurements cannot distinguish between the two different initial states, and $\chi = 1$. In the area law phase $\chi < 1$. For circuits with Clifford gates, we provide numerical evidence that χ can be sampled to accuracy ε from $O(1/\varepsilon^2)$ trajectories, by running the first circuit on a quantum simulator *without postselection*, aided by a classical simulation of the second. We also find that for weak depolarizing noise the signature of the measurement-induced phase transitions is still present for intermediate system sizes. In our protocol we have the freedom of choosing initial states such that the "classical" side can be simulated efficiently, while simulating the "quantum" side is still classically hard.

DOI: 10.1103/PhysRevLett.130.220404

Introduction.—Open quantum dynamics can host a rich phenomenology, including a family of measurement-induced phase transitions (MIPTs) in the scaling of entanglement along quantum trajectories in monitored systems [1–7]. The MIPT is a basic phenomenon in many-body quantum dynamics and occurs generically in a number of different models [8–26], yet its experimental observation can be challenging, even on an error-corrected quantum computer, due to the so-called "postselection problem." Quantum trajectories are labeled by the measurement history $\boldsymbol{m}$, whose length is extensive in the spacetime volume V of the circuit; thus, the number of possible trajectories $\boldsymbol{m}$ is exponential in V, but they each occur with roughly the same probability. On the other hand, one needs multiple copies of the same $\boldsymbol{m}$ in order to verify any quantum entanglement; and then many different $\boldsymbol{m}$ to perform a proper statistical average. On a quantum simulator there is no general recipe for producing such copies other than running the quantum circuit many times and waiting until the measurement results coincide ("postselection"). Naively, $O(e^V)$ runs of the circuit are required, thus severely restricting the scalability of such experiments. Nevertheless, in an impressive recent experiment that carries out postselection [27], the MIPT is observed on small scale superconducting quantum processors.

The exponential postselection overhead has previously been shown to be avoidable in two cases. First, when only Clifford circuits are considered, the entanglement can be verified by "decoding" the circuit, either through a full classical simulation within the stabilizer formalism [28] or via machine learning [29]. With machine learning the authors claim that "decoding" is possible also beyond Clifford circuits, although this has yet to be explored in detail. Second, when the nonunitary (monitored) dynamics is a spacetime dual of a unitary one [30–32], postselection is partially ameliorated, and correspondences between unitary dynamics and monitored dynamics can be made.

Here, we propose a resource efficient experimental protocol for verifying the MIPT in random circuits by estimating the "linear cross entropy" (denoted χ) between the probability distribution of (bulk circuit) measurement outcomes $\boldsymbol{m}$ in two circuits with the same bulk but different initial states, ρ and σ. Closely related quantities have been discussed previously [33]. In particular, as we establish, both numerically and analytically, in the thermodynamic limit the linear cross entropy (when suitably normalized) is 1 in the volume law phase, and equals a nonuniversal constant smaller than 1 in the area law phase. Thus, the MIPT can also be viewed as a phase transition in the distinguishability of two initial states, when the bulk measurement outcomes are given. In particular, the two initial states become essentially indistinguishable when measurements are below a critical density.

The definition of χ includes contributions from all samples of $\boldsymbol{m}$, and to estimate χ no postselection is involved. However, as we discuss below, estimating χ usually requires an exponentially long classical simulation, thus not scalable. Below, we show that when the classical simulation becomes scalable in Clifford circuits, χ can be efficiently sampled by running the ρ circuit on a quantum

simulator, aided by a classical simulation of the σ circuit. We provide numerical evidence that χ is an order parameter for the MIPT (i.e., $\chi = 1$ in the volume law phase and $\chi < 1$ in the area law phase).

By choosing the circuit bulk to be composed of Clifford operations and σ to be a stabilizer state, the protocol is scalable on both the quantum and the classical sides. Nevertheless, unless ρ is also a stabilizer state, the ρ circuit output state is still highly nontrivial and hard to represent classically. More broadly, our protocol represents a general —although not always scalable—approach for experimental observations of measurement-induced physics that does not reduce the quantum simulation to a mere confirmation of a classical computation; see recent examples in Refs. [36–39].

In [35] we consider one nontrivial aspect of the output state in the volume law phase when the ρ circuit is not efficiently classically simulable, namely the bistring distribution when all qubits are measured, and found qualitative differences from the Porter-Thomas distribution.

Linear cross entropy and order parameter.—We consider the "hybrid" circuit shown in Fig. 1, composed of unitary gates on nearest-neighbor qubits arranged in a brickwall structure, and single-site measurements in the bulk, performed with probability p at each qubit within each time step. By convention, each time step contains $L/2$ unitary gates. Different from the usual setup [9], we have an additional "encoding" stage before the hybrid evolution for time $t_{\text{encoding}} = 2L$, following Refs. [5,34]. The reason for this somewhat unusual choice is practical: to get a clearer experimental signal of the MIPT [35]. We call the evolution after the encoding stage the "circuit bulk," which lasts for another $t_{\text{bulk}} = 2L$. The total circuit time is $T = t_{\text{encoding}} + t_{\text{bulk}} = 4L$.

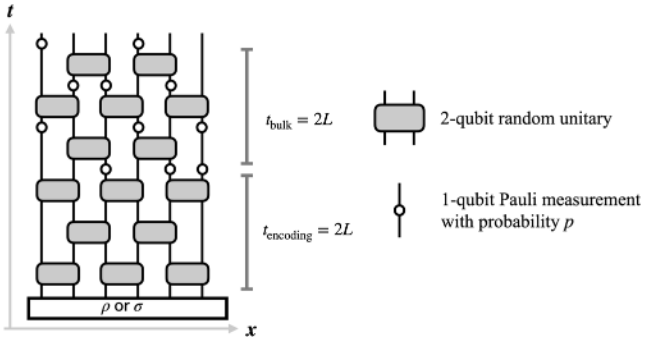

FIG. 1. The layout of the hybrid circuit considered in this Letter. Different from the usual setup [9], we have an additional "encoding" stage before the hybrid evolution for time $t_{\text{encoding}} = 2L$, following Ref. [5]. We call the evolution after the encoding stage the "circuit bulk," which lasts for another $t_{\text{bulk}} = 2L$. The total circuit time is $T = t_{\text{encoding}} + t_{\text{bulk}} = 4L$. We will compare two different initial states ρ and σ (left unspecified for the moment) undergoing the same circuit evolution.

For concreteness, we take all the measurements to be in the Pauli Z basis. Given a circuit layout (as determined by the brickwork structure and the location of measurements) and the unitary gates in the bulk—which we denote collectively as C—the *unnormalized* output state is defined by C and the measurement record $\boldsymbol{m} = \{m_1, m_2, \ldots, m_N\}$ as

$$\rho_{\boldsymbol{m}} = C_{\boldsymbol{m}} \rho C_{\boldsymbol{m}}^{\dagger}, \tag{1}$$

where ρ is the initial state of the circuit, and $C_{\boldsymbol{m}}$ is the time-ordered product of all the unitaries and projectors in the circuit, written schematically as

$$C_{\boldsymbol{m}} = P_{m_N} P_{m_{N-1}} \ldots P_{m_{N-N_T+1}} \cdot U_T \cdot P_{m_{N-N_T}} \ldots P_{m_{N-N_T-N_{T-1}+1}} \cdot U_{T-1} \cdot P_{m_{N-N_T-N_{T-1}}} \ldots P_{m_{N-N_T-N_{T-1}-N_{T-2}+1}} \cdot U_{T-2} \ldots \tag{2}$$

Here, each line contains all quantum operations in one circuit time step, and N is the total number of measurements, which is proportional to the spacetime volume of the circuit $N \propto pV = pLT$. The corresponding probability of obtaining $\boldsymbol{m}$ is given by

$$p_{\boldsymbol{m}}^{\rho} = \mathrm{tr}\rho_{\boldsymbol{m}}. \tag{3}$$

We define similar quantities for a different initial state σ,

$$\sigma_{\boldsymbol{m}} = C_{\boldsymbol{m}} \sigma C_{\boldsymbol{m}}^{\dagger}, \tag{4}$$

$$p_{\boldsymbol{m}}^{\sigma} = \mathrm{tr}\sigma_{\boldsymbol{m}}. \tag{5}$$

With these, we define the (normalized) linear cross entropy of the circuit between the two initial states as

$$\chi_C = \frac{\sum_{\boldsymbol{m}} p_{\boldsymbol{m}}^{\rho} p_{\boldsymbol{m}}^{\sigma}}{\sum_{\boldsymbol{m}} (p_{\boldsymbol{m}}^{\sigma})^2}. \tag{6}$$

Here, for fixed choices of ρ and σ, after averaging over $\boldsymbol{m}$, χ_C only depends on the circuit C, and we have explicitly included this dependence in our notation (while keeping the dependence on ρ and σ implicit). Finally, we take its average over C,

$$\chi := \mathbb{E}_C \chi_C = \mathbb{E}_C \frac{\sum_{\boldsymbol{m}} p_{\boldsymbol{m}}^{\rho} p_{\boldsymbol{m}}^{\sigma}}{\sum_{\boldsymbol{m}} (p_{\boldsymbol{m}}^{\sigma})^2}. \tag{7}$$

It was previously pointed out [7] that a quantity closely related to $-\ln\chi$ corresponds to the free energy cost after fixing a boundary condition in a (replicated) spin model [6,7,40,41]; in [35], we provide a similar calculation for our

circuit. From this derivation we expect $1-\chi = e^{-O(L)}$ for large L in the volume law phase ($p < p_c$), and $1-\chi > 0$ in the area law phase ($p > p_c$), even as $L \to \infty$.

The physical meaning of χ is clear: it quantifies the difference between the probability distributions over measurement histories for the two initial states. In the volume law phase, $\chi = 1$ implies the impossibility of distinguishing different initial states from bulk measurements due to the "coding" properties of this phase (i.e., the dynamics in the volume law phase generates a "dynamical quantum memory" [4,5,42–45]). Intuitively, in the volume law phase, local measurements are so infrequent that it extracts little information about the initial state, as the information is sufficiently scrambled by the random unitaries. The code breaks down when p is increased past the transition, and χ saturates to a finite, nonuniversal constant strictly smaller than 1. In this phase, information about the initial state leaks into the measurement outcomes.

We now outline a protocol for estimating χ, which is similar to the linear cross entropy benchmark for random unitary circuits [46,47]. Then we discuss its limitations when applied to the MIPT and how to overcome them in case of a stabilizer circuit.

General setup.—Consider running the circuit with initial state ρ ("the ρ circuit") on a quantum simulator. From the simulation we obtain a measurement record $\boldsymbol{m}$, an event that occurs with probability $p^{\rho}_{\boldsymbol{m}}$. Given $\boldsymbol{m}$ we can perform a classical simulation with the initial state σ, and calculate the corresponding probability $p^{\sigma}_{\boldsymbol{m}}$. Repeating this M times, we obtain a sequence of probabilities $\{p^{\sigma}_{\boldsymbol{m}_1}, p^{\sigma}_{\boldsymbol{m}_2}, \ldots p^{\sigma}_{\boldsymbol{m}_M}\}$. Their mean converges to the numerator of Eq. (6):

$$\lim_{M\to\infty} \langle p^{\sigma}_{\boldsymbol{m}^M_{j=1}} \rangle_{\rho} \coloneqq \lim_{M\to\infty} \frac{1}{M}\sum_{j=1}^{M} p^{\sigma}_{\boldsymbol{m}_j} = \sum_{\boldsymbol{m}} p^{\rho}_{\boldsymbol{m}} p^{\sigma}_{\boldsymbol{m}}. \quad (8)$$

The denominator of Eq. (6) can be estimated similarly, with a separate classical simulation, by running the σ circuit M' times and computing the mean of probabilities $\{p^{\sigma}_{\boldsymbol{m}_j}\}$. This way we get

$$\lim_{M'\to\infty} \langle p^{\sigma}_{\boldsymbol{m}^{M'}_{j=1}} \rangle_{\sigma} \coloneqq \lim_{M'\to\infty} \frac{1}{M'}\sum_{j=1}^{M'} p^{\sigma}_{\boldsymbol{m}_j} = \sum_{\boldsymbol{m}} (p^{\sigma}_{\boldsymbol{m}})^2. \quad (9)$$

Both equations above are well-defined, and in this protocol each run of the circuit is used, so no postselection is required. This should lead to a general protocol for experimentally probe MIPTs, although a full classical simulation is still necessary, and the experimentally accessible system size will be limited by the power of classical simulation.

To obtain a scalable protocol, we first focus on the case where σ is a stabilizer state, and the circuit bulk $C_{\boldsymbol{m}}$ is composed of stabilizer operations (Clifford gates and Pauli measurements) [48–50]. At this point we do not put constraint on ρ. In this special case, the denominator of Eq. (6) can be computed exactly in polynomial time, without doing any sampling as in Eq. (9) [35]. Thus, we may rewrite Eq. (6) as

$$\chi_C = \sum_{\boldsymbol{m}} p^{\rho}_{\boldsymbol{m}} \frac{p^{\sigma}_{\boldsymbol{m}}}{\sum_{\boldsymbol{m}} (p^{\sigma}_{\boldsymbol{m}})^2}, \quad (10)$$

and in analogy with Eq. (8),

$$\chi_C = \lim_{M\to\infty} \left\langle \frac{p^{\sigma}_{\boldsymbol{m}^M_{j=1}}}{\sum_{\boldsymbol{m}} (p^{\sigma}_{\boldsymbol{m}})^2} \right\rangle_{\rho}. \quad (11)$$

For each run of the ρ circuit, we obtain the measurement record $\boldsymbol{m}_j$ and compute $[p^{\sigma}_{\boldsymbol{m}_j}/\sum_{\boldsymbol{m}} (p^{\sigma}_{\boldsymbol{m}})^2]$ in polynomial time, and take its mean over runs. Since the circuit is Clifford, the new "observable" $[p^{\sigma}_{\boldsymbol{m}_j}/\sum_{\boldsymbol{m}} (p^{\sigma}_{\boldsymbol{m}})^2]$ is either 0 or 1 for a given $\boldsymbol{m}$ [35], and this average converges quickly with increasing M. In particular, since this is a binary random variable, the variance of the samples should decay as $M^{-1/2}$ for a given C. Thus, for a fixed circuit M scales as $1/\varepsilon^2$, where ε is the error of the estimation of χ_C. We also see that χ_C is always bounded between 0 and 1. This is a property special to Clifford circuits.

Numerical methods and results.—We first take ρ to be a stabilizer state, while keeping σ another stabilizer state. As we explain in [35] now χ_C in Eq. (10) admits a closed form expression that does not involve any summation over $\boldsymbol{m}$. This allows an exact calculation of χ_C without the need of performing any sampling, at the cost of introducing N extra qubits that record the measurement history. These qubits are usually called "registers."

A further simplification occurs when ρ is obtainable from σ via erasure or dephasing channels, so that the N register qubits can also be dispensed with [35]. We will focus on this case below, where the numerical simulation is most scalable so that we can confidently extrapolate the results to more general choices of ρ.

In Fig. 2(a), we plot $\chi = \mathbb{E}_C \chi_C$ for $\rho = (1/2^L)\mathbb{1}$ and $\sigma = (|0\rangle\langle 0|)^{\otimes L}$, which satisfies the condition above. The data show a clear "crossing" of χ near the transition, confirming our expectation that χ is an order parameter for the MIPT. Indeed, in the large L limit and for $p < p_c$, χ approaches unity, demonstrating that the distributions of measurement outcomes become equal, independent of the initial state. Moreover, data collapse in Fig. 2(d) shows good agreement to a standard scaling form, with numerical values of the location of the transition p_c and of the critical exponent ν close to previous characterizations of the MIPT [9].

An important practical parameter is the number M_C [51] of circuit samples needed to estimate χ within a given accuracy, in particular their scaling with the system size. By the central limit theorem, given independent samples

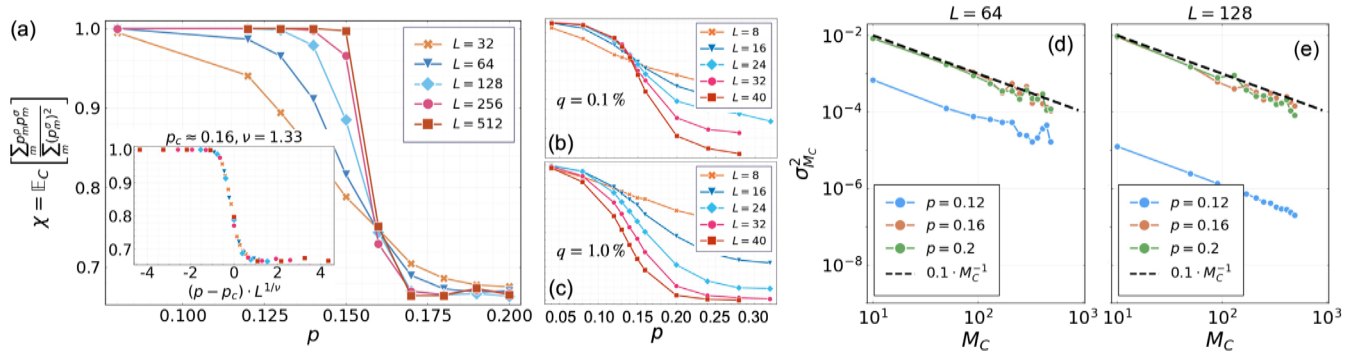

FIG. 2. (a) Numerical results for χ_C when averaged over 300 Clifford circuits in the bulk (denoted by $\mathbb{E}_C$), with the initial states $\rho = (1/2^L)\mathbb{1}$ and $\sigma = (|0\rangle\langle 0|)^{\otimes L}$. Here, for each C, the calculation is exact, and M can be thought of as infinity in Eq. (11). Inset: collapsing the data to a scaling form, with parameters p_c and ν close to those found near the MIPT in entanglement entropy [3,9]. (b),(c) The behavior of χ when depolarizing noise is present in the ρ circuit. As we see, at noise rate $q = 0.1\%$ (b), there is still evidence for a phase transition, although the location of the transition has shifted from $p_c \approx 0.16$ to $p_c \approx 0.14$. At noise rate 1% (c), there is no crossing, and any signature of the phase transition is completely washed out. (d),(e) The convergence of the sample average $\mu_{M_C} = (M_C)^{-1}\sum_{j=1}^{M_C}\chi_{C_j}$ to $\chi = \mathbb{E}_C\chi_C$ with increasing number of circuit samples M_C. For each of $L \in \{64, 128\}$, we plot $\sigma^2_{M_C} = \mathbb{E}[(\mu_{M_C} - \chi)^2]$ for $M_C \leq 500$, whereas χ is estimated using $M_C = 2000$ circuits. The results are consistent with the central limit theorem; see Eq. (12). From this plot we see that sample variance is suppressed by large L when $p < p_c$, and is independent of L when $p \geq p_c$. This justifies our choice of a relatively small M_C that is independent of the system size.

$\{C_{j=1}^{M_C}\}$, the sample average $\mu_{M_C} = (1/M_C)\sum_{j=1}^{M_C}\chi_{C_j}$ converges to χ at large M_C as follows:

$$\sigma^2_{M_C} = \mathbb{E}[(\mu_{M_C} - \chi)^2] \propto (M_C)^{-1}, \tag{12}$$

with an overall amplitude that converges to the variance of χ_C, $\sigma^2[\chi_C] \coloneqq \mathbb{E}_C[\chi_C^2] - (\mathbb{E}_C[\chi_C])^2$. In Figs. 2(d) and 2(e) we compute $\sigma^2_{M_C}$ numerically at two different system sizes L and at different locations of the phase diagram. Our results confirm Eq. (12), and by fitting the overall amplitude we find that $\sigma^2[\chi_C]$ is suppressed by large L in the volume law phase $p < p_c$ (as consistent with $\chi \to 1$), and saturates to an L-independent constant (≈ 0.1) for $p \geq p_c$. Together with our previous discussion on M (number of runs per circuit C), these results justify our choices of relatively small M_C and M that are independent of system sizes; see Figs. 2 and 3(a) below.

We also consider the effect of depolarizing noise occurring randomly in the ρ circuit with probability q per qubit per time step, whereas the σ circuit is still taken to be noiseless. The setup is to mimic an experimental sampling procedure where we run the ρ circuit on a quantum processor subject to noise, whereas our supplemental classical simulation of the σ circuit is noiseless. The depolarizing noise acts as a symmetry-breaking field in the effective spin model [6,7,30,31,52–55] and in its presence the MIPT is no longer sharply defined. Nevertheless, evidence of the MIPT may still be observable if the error rate is small compared to the inverse spacetime volume of the circuit, as we see in Figs. 2(b) and 2(c).

Next, we take ρ to be a nonstabilizer state, and σ to be a stabilizer state. In particular, we choose a state with $|0\rangle$ and $|T\rangle$ on alternating sites, $\rho = \otimes_{i=1}^{L/2}(|0\rangle\langle 0|_{2i-1} \otimes |T\rangle\langle T|_{2i})$, where $|T\rangle = (1/\sqrt{2})(|0\rangle + e^{i\pi/4}|1\rangle)$ is a magic state. We still take the other initial state to be $\sigma = (|0\rangle\langle 0|)^{\otimes L}$.

Based on our calculations [35], we expect χ_C to exhibit similar behavior as in Fig. 2. This is confirmed in Fig. 3(a), where we follow the sampling procedure in Eq. (11). In particular, for a given C, we take $L \in \{8, 12, 16\}$, and sample $M = 100$ measurement trajectories, and compute

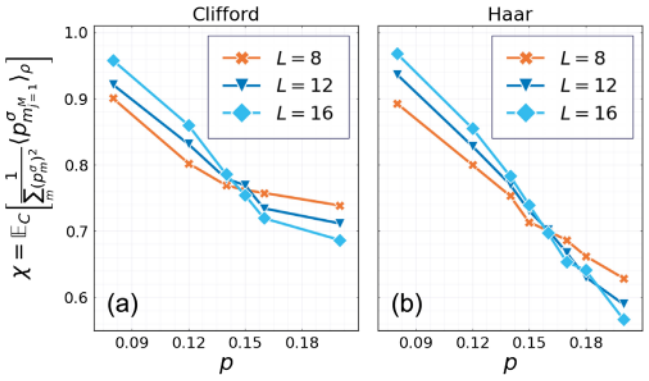

FIG. 3. (a) Numerical results of χ for initial states $\rho = \otimes_{i=1}^{L/2}(|0\rangle\langle 0|_{2i-1} \otimes |T\rangle\langle T|_{2i})$ and $\sigma = (|0\rangle\langle 0|)^{\otimes L}$ obtained from random Clifford circuits. Here, $M_C = 300$ circuit realizations are taken for each L, and for each circuit, we use $M = 100$ runs to estimate χ_C, following Eq. (11). Compared to Fig. 2(a), the results are qualitatively similar, despite a different choice of initial state and smaller system sizes. (b) Numerical results of χ for initial states $\rho = (|+\rangle\langle +|)^{\otimes L}$ and $\sigma = (|0\rangle\langle 0|)^{\otimes L}$ obtained from random Haar circuits. Here, $M_C = 150$ circuit realizations are taken for each L, and for each circuit we estimate Eqs. (8) and (9) separately, using $M = 3200$ runs each.

$\langle p^{\sigma}_{\boldsymbol{m}^M_{j=1}} / \sum_{\boldsymbol{m}} (p^{\sigma}_{\boldsymbol{m}})^2 \rangle_{\rho} \approx \chi_C$. We then take the average over many different choices of C, namely $\mathbb{E}_C \langle p^{\sigma}_{\boldsymbol{m}^M_{j=1}} / \sum_{\boldsymbol{m}} (p^{\sigma}_{\boldsymbol{m}})^2 \rangle_{\rho} \approx \mathbb{E}_C \chi_C$. We observe a crossing of χ at roughly the same value of p_c in Fig. 2(a). The system sizes that we accessed are limited by classical simulations of the ρ circuit [59], but we hope larger system sizes can be achieved on near-term quantum processors.

Finally, to test the validity of our approach beyond Clifford circuits, we calculate χ in circuits with random Haar unitary gates for $\rho = (|+\rangle\langle+|)^{\otimes L}$ and $\sigma = (|0\rangle\langle 0|)^{\otimes L}$. Here, we have to estimate the normalization of χ_C [see Eqs. (6) and (9)] separately. To obtain plots with comparable accuracy as those from Clifford circuits, the number of runs per circuit needs to be at least an order of magnitude larger (for system sizes up to $L = 16$) due to the additional numerical uncertainty in the normalization. Our results are shown in Fig. 3(b), with an overall trend consistent with a phase transition.

Discussions.—Our protocol requires a simulation of many instances of the random hybrid circuit with mid-circuit measurements, and for each instance $O(1/\varepsilon^2)$ trajectories to estimate the cross entropy to accuracy ε. This should be a task of similar complexity to Google's simulation of random unitary circuits [47], except that here we do not make measurements on the output state but in the bulk. However, different from that experiment, for observing the MIPT it suffices to focus on Clifford circuits, for which the classical simulation is not hard. This protocol is thus as scalable as the quantum processors. Our protocol does not require extra quantum operations, and is flexible in the choice of the initial state. The signal for the phase transition persists at $L = 40$ for sufficiently weak ($\approx 0.1\%$) depolarizing noise. Thus, we hope this protocol might be achievable on existing or near-term devices.

If the circuit is not composed of Clifford gates, our protocol is expected to require exponential classical resources. It is presently unclear whether it is in fact possible to probe the MIPT beyond Clifford circuits with polynomial resources [29].

Although the classical simulation is chosen to be easy for practical purposes, in our protocol the quantum simulation is classically hard for a generic choice of the initial state, which would result in a highly nontrivial output state. Our numerical results in [35] suggest that sampling measurement outcomes on the output state of the quantum simulation is classically hard in the volume law phase. Whether this can be used in practice for demonstrating quantum advantage is not known, due to apparent need of postselection in order to sample from this distribution.

We acknowledge helpful discussions with Tanvi Gujarati, Jacob Hauser, Hirsh Kamakari, Vedika Khemani, Jin Ming Koh, Ali Lavasani, Austin Minnich, Mario Motta, Alan Morningstar, Xiao-Liang Qi, Shi-Ning Sun, Shengqi Sang, Jonathan Thio, Sagar Vijay, and Sisi Zhou. We thank Michael Gullans and Edward Chen for useful suggestions, and Matteo Ippoliti for pointing out a mistake in an earlier version of the Supplemental Material [35]. Y. L. is grateful for the hospitality of Vedika Khemani at Stanford University, where much of this work was undertaken. This work was supported by the Heising-Simons Foundation (Y. L. and M. P. A. F.), and by the Simons Collaboration on Ultra-Quantum Matter, which is a grant from the Simons Foundation (651457, M. P. A. F.). Y. Z. is supported by the Q-FARM fellowship at Stanford University. P. G. is supported by the Alfred P. Sloan Foundation through Grant No. FG-2020-13615, the Department of Energy through Award No. DE-SC0019380, and the Simons Foundation through Grant No. 620869. E. A. is supported in part by the NSF QLCI program through Grant No. OMA-2016245. Use was made of computational facilities purchased with funds from the National Science Foundation (CNS-1725797) and administered by the Center for Scientific Computing (CSC). The CSC is supported by the California NanoSystems Institute and the Materials Research Science and Engineering Center (MRSEC; NSF DMR-1720256) at UC Santa Barbara.

[1] B. Skinner, J. Ruhman, and A. Nahum, Phys. Rev. X **9**, 031009 (2019).
[2] A. Chan, R. M. Nandkishore, M. Pretko, and G. Smith, Phys. Rev. B **99**, 224307 (2019).
[3] Y. Li, X. Chen, and M. P. A. Fisher, Phys. Rev. B **98**, 205136 (2018).
[4] S. Choi, Y. Bao, X.-L. Qi, and E. Altman, Phys. Rev. Lett. **125**, 030505 (2020).
[5] M. J. Gullans and D. A. Huse, Phys. Rev. X **10**, 041020 (2020).
[6] C.-M. Jian, Y.-Z. You, R. Vasseur, and A. W. W. Ludwig, Phys. Rev. B **101**, 104302 (2020).
[7] Y. Bao, S. Choi, and E. Altman, Phys. Rev. B **101**, 104301 (2020).
[8] X. Cao, A. Tilloy, and A. De Luca, SciPost Phys. **7**, 024 (2019).
[9] Y. Li, X. Chen, and M. P. A. Fisher, Phys. Rev. B **100**, 134306 (2019).
[10] M. Szyniszewski, A. Romito, and H. Schomerus, Phys. Rev. B **100**, 064204 (2019).
[11] Q. Tang and W. Zhu, Phys. Rev. Res. **2**, 013022 (2020).
[12] A. Nahum and B. Skinner, Phys. Rev. Res. **2**, 023288 (2020).
[13] J. Lopez-Piqueres, B. Ware, and R. Vasseur, Phys. Rev. B **102**, 064202 (2020).
[14] A. Lavasani, Y. Alavirad, and M. Barkeshli, Nat. Phys. **17**, 342 (2021).
[15] S. Sang and T. H. Hsieh, Phys. Rev. Res. **3**, 023200 (2021).
[16] M. Ippoliti, M. J. Gullans, S. Gopalakrishnan, D. A. Huse, and V. Khemani, Phys. Rev. X **11**, 011030 (2021).
[17] X. Chen, Y. Li, M. P. A. Fisher, and A. Lucas, Phys. Rev. Res. **2**, 033017 (2020).
[18] Y. Fuji and Y. Ashida, Phys. Rev. B **102**, 054302 (2020).

[19] O. Alberton, M. Buchhold, and S. Diehl, Phys. Rev. Lett. **126**, 170602 (2021).
[20] O. Lunt and A. Pal, Phys. Rev. Res. **2**, 043072 (2020).
[21] S. Vijay, arXiv:2005.03052.
[22] X. Turkeshi, R. Fazio, and M. Dalmonte, Phys. Rev. B **102**, 014315 (2020).
[23] A. Nahum, S. Roy, B. Skinner, and J. Ruhman, PRX Quantum **2**, 010352 (2021).
[24] Y. Bao, S. Choi, and E. Altman, Ann. Phys. (Amsterdam) **435**, 168618 (2021).
[25] U. Agrawal, A. Zabalo, K. Chen, J. H. Wilson, A. C. Potter, J. H. Pixley, S. Gopalakrishnan, and R. Vasseur, Phys. Rev. X **12**, 041002 (2022).
[26] F. Barratt, U. Agrawal, S. Gopalakrishnan, D. A. Huse, R. Vasseur, and A. C. Potter, Phys. Rev. Lett. **129**, 120604 (2022).
[27] J. M. Koh, S.-N. Sun, M. Motta, and A. J. Minnich, arXiv:2203.04338.
[28] C. Noel, P. Niroula, D. Zhu, A. Risinger, L. Egan, D. Biswas, M. Cetina, A. V. Gorshkov, M. J. Gullans, D. A. Huse, and C. Monroe, Nat. Phys. **18**, 760 (2022).
[29] H. Dehghani, A. Lavasani, M. Hafezi, and M. J. Gullans, Nat. Commun. **14**, 2918 (2023).
[30] M. Ippoliti and V. Khemani, Phys. Rev. Lett. **126**, 060501 (2021).
[31] M. Ippoliti, T. Rakovszky, and V. Khemani, Phys. Rev. X **12**, 011045 (2022).
[32] T.-C. Lu and T. Grover, PRX Quantum **2**, 040319 (2021).
[33] In particular, Ref. [7] proposed the Fisher information, quantifying the change in the bulk measurement outcome distribution when the initial state is slightly perturbed. Reference [34] proposed the entropy of a reference qubit as a boundary order parameter, where the reference qubit is initially maximally entangled with the system and gets purified under measurements. Both quantities are are akin to a boundary magnetization, although in a different stat mech model, as we discuss in the Supplemental Material [35]. Reference [34] also considered the purification a reference qubit after an encoding stage is applied in a way similar to Fig. 1.
[34] M. J. Gullans and D. A. Huse, Phys. Rev. Lett. **125**, 070606 (2020).
[35] See Supplemental Material at http://link.aps.org/supplemental/10.1103/PhysRevLett.130.220404 for discussions of the cross entropy in an effective spin model, the encoding stage of the circuit, the numerical algorithm for estimating the cross entropy in Clifford circuits, and the bistring distribution function in the output state.
[36] S. J. Garratt, Z. Weinstein, and E. Altman, Phys. Rev. X **13**, 021026 (2023).
[37] X. Feng, B. Skinner, and A. Nahum, arXiv:2210.07264.
[38] Z. Weinstein, R. Sajith, E. Altman, and S. J. Garratt, arXiv:2301.08268 [Phys. Rev. B (to be published)].
[39] F. Barratt, U. Agrawal, A. C. Potter, S. Gopalakrishnan, and R. Vasseur, Phys. Rev. Lett. **129**, 200602 (2022).
[40] A. Nahum, S. Vijay, and J. Haah, Phys. Rev. X **8**, 021014 (2018).
[41] T. Zhou and A. Nahum, Phys. Rev. B **99**, 174205 (2019).
[42] R. Fan, S. Vijay, A. Vishwanath, and Y.-Z. You, Phys. Rev. B **103**, 174309 (2021).
[43] Y. Li and M. P. A. Fisher, Phys. Rev. B **103**, 104306 (2021).
[44] L. Fidkowski, J. Haah, and M. B. Hastings, Quantum **5**, 382 (2021).
[45] B. Yoshida, arXiv:2109.08691.
[46] S. Boixo, S. V. Isakov, V. N. Smelyanskiy, R. Babbush, N. Ding, Z. Jiang, M. J. Bremner, J. M. Martinis, and H. Neven, Nat. Phys. **14**, 595 (2018).
[47] F. Arute *et al.*, Nature (London) **574**, 505 (2019).
[48] D. Gottesman, Stabilizer codes and quantum error correction, Ph.D. thesis, California Institute of Technology, 1997, arXiv:quant-ph/9705052.
[49] D. Gottesman, arXiv:quant-ph/9807006.
[50] S. Aaronson and D. Gottesman, Phys. Rev. A **70**, 052328 (2004).
[51] Notice that this is *the number of samples of C* and is different from M as discussed above, which is *the number of runs (or trajectories) taken for each circuit sample C*. In this discussion we assume that $\{\chi_{C_{j=1}^{M_C}}\}$ have been obtained following previous discussions around Eq. (11), when M is taken to infinity.
[52] Y. Li, X. Chen, A. W. W. Ludwig, and M. P. A. Fisher, Phys. Rev. B **104**, 104305 (2021).
[53] Y. Li, S. Vijay, and M. P. A. Fisher, PRX Quantum **4**, 010331 (2023).
[54] S.-K. Jian, C. Liu, X. Chen, B. Swingle, and P. Zhang, arXiv:2106.09635.
[55] See also Refs. [56–58] for related discussion in random unitary circuits.
[56] K. Noh, L. Jiang, and B. Fefferman, Quantum **4**, 318 (2020).
[57] A. Deshpande, P. Niroula, O. Shtanko, A. V. Gorshkov, B. Fefferman, and M. J. Gullans, PRX Quantum **3**, 040329 (2022).
[58] A. M. Dalzell, N. Hunter-Jones, and F. G. S. L. Brandáo, arXiv:2111.14907.
[59] S. Bravyi and D. Gosset, Phys. Rev. Lett. **116**, 250501 (2016).